

Hydrodynamics of Internal Shocks in Relativistic Outflows

M. Kino^{*}, A. Mizuta[†], A. Celotti^{*} and S. Yamada^{**}

^{*}*SISSA, via Beirut 2-4, 34014 Trieste, Italy*

[†]*Yukawa Institute for Theoretical Physics, Kyoto University, Kyoto 606-8502, Japan*

^{**}*Science and Engineering, Waseda University, Shinjyuku, Tokyo 169-8555, Japan*

Abstract. We study the hydrodynamical effects of two colliding shells, adopted to model internal shocks in various relativistic outflows such as gamma-ray bursts and blazars. We find that the density profiles are significantly affected by the propagation of rarefaction waves. A split-feature appears at the contact discontinuity of the two shells. The shell spreading with a few ten percent of the speed of light is also shown to be a notable aspect. The conversion efficiency of the bulk kinetic energy to internal one shows deviations from the widely-used inelastic two-point-mass-collision model. Observational implications are also shortly discussed.

INTRODUCTION

The internal shock scenario proposed by Rees (1978) is one of the most promising models to explain the observational features of relativistic outflows associated to e.g., gamma-ray bursts, and blazars (e.g., Rees & Meszaros 1992; Spada et al. 2001). Most of the previous works focus on the comparison of the model predictions employing a simple inelastic collision of two point masses with observed light curves (e.g., Kobayashi et al. 1997; Daigne & Mochkovitch 1998) and little attention has been paid to hydrodynamical processes in the shell collision. However, it is obvious that, in the case of relativistic shocks, the time scales in which shock and rarefaction waves cross the shells are comparable to the dynamical time scale Δ'/c , where Δ' is the shell width measured in the comoving frame of the shell and c is the speed of light. Since the time scales of observations of these relativistic outflows (e.g., Takahashi et al. 2000 for blazar jet; Fishman & Meegan 1995 for GRBs) are much longer than the dynamical one, the light curves should contain the footprints of these hydrodynamical wave propagations. Thus, it is worth to study the difference between the simple two-point-mass-collision (hereafter two-mass-collision) model and the hydrodynamical treatment. Here we show (1) the hydrodynamical effects, especially including the propagations of rarefaction wave (Kino, Mizuta & Yamada 2004 hereafter KMY) and (2) some implications of hydrodynamical model on the observed phenomena.

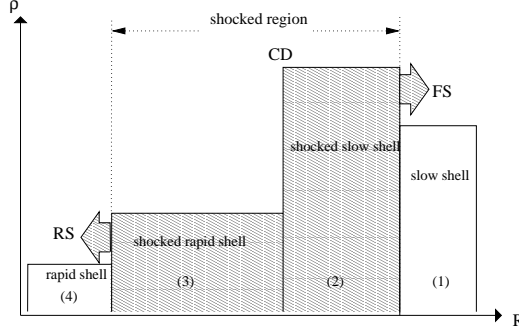


FIGURE 1. Sketch of a two-shell-collision where a rapid shell catches up with a slower one in the contact discontinuity (CD) rest frame (hereafter CD frame). Forward and reverse shocks (FS and RS) propagate from the CD. We adopt the conventional numbering for each region used in the study of GRB (e.g., Piran 1999).

INTERNAL SHOCK MODEL

Here we consider the hydrodynamics of the two-shell interaction (the fundamental physics of relativistic shocks can be found in Landau & Lifshitz 1959 and Blandford & McKee 1976). Our main assumptions are (1) adopt a planar 1D shock and neglect radiative cooling for simplicity, (2) neglect the effect of magnetic fields, and (3) limit our attention to shells with relativistic speeds.

In Fig. 1, we draw a schematic mass density profile of the shock propagation during the interaction of a rapid (fast) and a slow shell. Two shocks are formed: a reverse shock (RS) that moves into the rapid shell and a forward shock (FS) that propagates into the slow one. There are four characteristic regions: (1) the unshocked slow shell, (2) the shocked slow shell, (3) the shocked rapid shell, and (4) the unshocked rapid shell. Thermodynamic quantities, such as rest mass density ρ , pressure P , and internal energy density e are measured in the fluid rest frames. We use the terminology of *regions* i ($i=1, 2, 3$, and 4) and *position of discontinuity* j ($j=FS, CD$, and RS) where CD stands for a contact discontinuity. The fluid velocity and Lorentz factor in the region i measured in the ISM rest frame are expressed as β_{ic} , and Γ_i , respectively. Throughout this work, we use the assumption of $\Gamma_i \gg 1$.

We perform special relativistic hydrodynamical simulations. The details of the code are given in Mizuta et al. (2004) and references therein. We assume plane symmetry and consider the one dimensional motions of shells. In discussing the propagation of shock and rarefaction waves, we choose the CD frame. We start the calculation at $t = 0$ when the collision of two shells has just begun. In this work, we set $\Delta'_s/c = 1$ and $\rho_r = 1$ as units of the numerical simulations. The subscripts r and s represent rapid and slow shells, respectively. As for an equation of state (EOS), we set an adiabatic index $\hat{\gamma}_i = 5/3$ for non-relativistic case and $\hat{\gamma}_i = 4/3$ for relativistic case, respectively. Initially, two shells have opposite velocities, namely, $\beta'_r > 0$ and $\beta'_s < 0$. We assume that the boundary of each shell is kept intact during the passage of shocks and rarefaction waves (i.e. we do not impose any condition for the plasma surrounding the two shells).

Bearing in mind the application to relativistic outflows in GRBs and blazars, we

assume that the widths of two shells are the same in the ISM frame, i.e. $\Delta_r/\Delta_s = 1$ (see, e.g., Nakar & Piran 2002 hereafter NP02). It seems natural to suppose that ejected shells from the central engine have a correlation among them. Here we consider following three cases; (1) the energy of bulk motion of the rapid shell ($E = \Gamma mc^2$) equals to that of the slow one in the ISM frame (we refer to it as “equal energy (or E)”), (2) the mass of rapid shell ($m = \rho\Gamma\Delta$) equals to that of the slow one (hereafter we call it “equal mass (or m)”), and (3) the rest mass density of rapid shell equals to that of the slow one (hereafter we call it “equal rest mass density (or ρ)”). Due to space limitations, we highlight, in this proceeding, the case of equal mass which satisfies $\rho_r\Delta_r\Gamma_r = \rho_s\Delta_s\Gamma_s$.

RESULTS

Shell “split” and “spread”

It is interesting to notice that, when the rarefaction wave from the FS side reaches the CD earlier than the one from the RS side, then the “split” occurs at the CD since the rarefaction wave going from the higher density region (region 2) into the lower density region (region 3) makes a dip in the latter region. The “split” feature is clearly seen in Figs. 2 and 3.

In principle, we can obtain the speed of the rarefaction wave using Riemann invariants. In the relativistic limit, it is known that the speed of the head of the rarefaction wave is close to the speed of light (e.g., Anile 1989). As the EOS of the shocked region deviates from the relativistic one, the speed is reduced. The head propagation is identified as the shell “spread” which appears in Figs. 2 and 3.

Energy conversion efficiency

The conversion efficiency of the bulk kinetic energy into internal one is a fundamental issue. The estimation of the energy conversion efficiencies with shock and rarefaction waves taken into account are presented in Fig. 4, on the basis of our 1D numerical simulations. By analogy with the two-mass-collision model, we define the efficiency measured in the ISM frame as

$$\varepsilon(t) \equiv 1 - \frac{\int \Gamma(t,x) dm(t,x)}{\Gamma_r m_r + \Gamma_s m_s} \quad (1)$$

where $dm(t,x)$, $\rho(t,x)$, $\Gamma(t,x)$, and $\Gamma(t,x)dx$, are the rest mass element, the rest mass density, and the Lorentz factor, measured in the ISM frame, and the length of the line element in the CD frame, respectively. In Fig. 4, we compare the numerical results with the predictions by the two-mass-collision approximation. After the shock waves break-out from the shells, the conversion efficiency is reduced by several 10% from the estimate of the two-mass-collision model after several dynamical times.

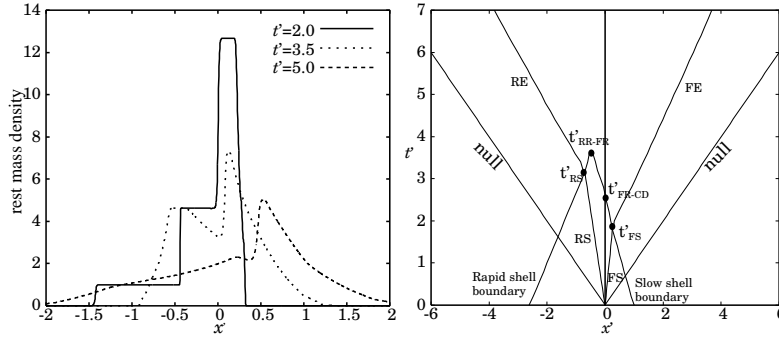


FIGURE 2. Left: Time evolution of the rest mass density profile in the CD frame for “equal m ”. In the ISM frame $\Gamma_r/\Gamma_s = 3$. The parameters are shown in Table 1. Space-time diagram of shock and rarefaction waves propagations. The rarefaction wave from the RS side (RE) spreads at the speed $\sim 0.8c$ while the one from FS side (FE) spreads at the speed $\sim 0.7c$.

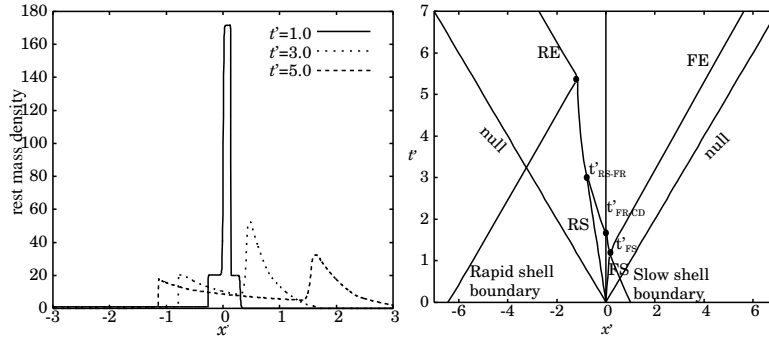


FIGURE 3. Left: Time evolution of the rest mass density profile in the CD frame for “equal m ”. In the ISM frame, $\Gamma_r/\Gamma_s = 20$. The parameters are shown in Table 1. The low density rapid shell collides with the slow one and quickly spreads out. We also see that the dense slow shock is pushed forward by the rapid shell. Right: Space-time diagram of shock and rarefaction waves propagations. RE spreads at the speed $\sim c$ while FE spreads at the speed $\sim 0.9c$.

Observational implications

It is worth discussing the hydrodynamic effects which may appear as observable features. Here we discuss (i) the pulse shape in light curves, and (ii) the energy conversion efficiency in multiple collisions.

TABLE 1. Parameter sets for numerical simulations of “equal m ”.

	Γ_r/Γ_s	Γ_{CD}^*	Γ'_r	Γ'_s	Δ'_r/Δ'_s	ρ_s/ρ_r
equal m (Fig.2)	3	7.6	1.25	1.09	2.6	3
equal m (Fig.3) [†]	20	11.8	4.29	1.40	6.4	20

* The slow shell Lorentz factor is fixed at $\Gamma_s = 5$.

[†] We use $\hat{\gamma}_3 = 4/3$.

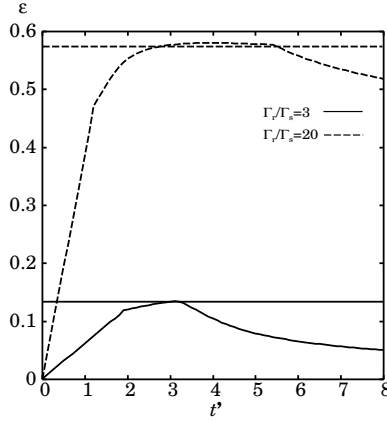


FIGURE 4. Time evolutions of the conversion efficiency defined by Eq. (1) for the “equal m ” case. During the shock propagations, ε approaches the constant values (horizontal lines) estimated by two-point-mass model.

On pulse shapes

A pulse shape is basically determined by the rising and decaying times. The relevant time scales that determine the pulse width are (e.g., Piran 1999 and references therein): (i) The angular time, t_{ang} , which results from the spherical geometry of the shells, (ii) The hydrodynamic time, t_{dyn} , which arises from the shell’s width and the shock crossing time, and (iii) The cooling time - the time that it takes for the emitting electrons to cool. If the cooling time is much shorter than t_{ang} and t_{dyn} , then no rarefaction wave is expected. The hydrodynamics effect may however come from the asymmetry of the crossing time of forward and reverse shocks. When the cooling time is comparable to t_{ang} and t_{dyn} , then rarefaction waves may play a significant role on the pulse shape. It is reasonable to suppose that the emission coming from the rarefaction wave zone contributes to observed light curves.

On the conversion efficiency

It is interesting to explore the conversion efficiency of the bulk kinetic energy into internal one within the context of a realistic multiple collision case. In Tanihata et al. (2002), the conversion efficiency of the internal shock scenario is assessed by evaluating the relative amplitude of flares as compared to the steady (“offset”) component. Given the duration of the ejected shells, the width of the pulse determines the height of the “offset” component. Wider width make the “offset” shorter. As mentioned above, the emission originating in the rarefaction wave is likely to contribute to each observed pulse in the weak cooling regime.

SUMMARY

We have studied 1D hydrodynamical simulations of two-shell-collisions in the CD frame. We find that rarefaction waves have a dramatic effect on the dynamics. Especially when a cooling time scale is sufficiently long in the shocked region, the observed emission may significantly be affected by them.

(1) In the case of “equal m ”, the profile should in principle become triple-peaked according to our classification scheme. In practice, however, there is very short time for two-rarefaction-waves (FR-RR) collision to produce a clear dip, while there is a lot more time for the FR to create a dip over a fairly wide range of parameters. Therefore, the profile in this case is effectively double-peaked (so-called shell “split”).

(2) For large Γ_r/Γ_s , the “spread” velocity of the shells after the collision is close to the speed of light. Hence, the often used approximation of constant shell width after collision is not very good in treating multiple collisions (e.g., NP02).

(3) The time-dependent energy conversion efficiency is quantitatively estimated. As the shell spreads after a collision, the internal energy is converted back into bulk kinetic energy due to thermal expansion. If $\Gamma_r/\Gamma_s \gg 1$ and the time-interval between collisions is long, the conversion efficiency will substantially deviate from the estimate of the two-mass-collision model.

ACKNOWLEDGMENTS

The work reported here was supported in part by Grand-in-Aid Program for Scientific Research (14340066, 14740166, and 14079202) from the Ministry of Education, Science, Sports, and Culture of Japan. M. K. and A. C. acknowledge the Italian MIUR and INAF financial support.

REFERENCES

1. Anile, A. M. 1989, *Relativistic Fluids and Magnetofluids*, Cambridge Univ. Press, Cambridge
2. Blandford, R. D. & McKee, C. F. 1976, *Physics of Fluids*, 19, 1130
3. Daigne F., Mochkovitch R., 1998, *MNRAS*, 296, 275
4. Fishman, G. J. & Meegan, C. A. 1995, *ARA&A*, 33, 415
5. Kino M., Mizuta A., & Yamada S., 2004, *ApJ*, 349, 1021 (KMY)
6. Kobayashi, S., Piran, T., & Sari, R. 1997, *ApJ*, 490, 92
7. Landau, L. D., & Lifshitz, E. M. 1959, *Fluid Mechanics*, Pergamon Press, Oxford
8. Mizuta, A., Yamada, S., & Takabe, H. 2004, *ApJ*, 606, 804
9. Nakar, E. & Piran, T. 2002, *ApJL*, 572, L139 (NP02)
10. Piran, T. 1999, *Phys. Rep.*, 314, 575
11. Rees, M. J. 1978, *MNRAS*, 184, 61
12. Rees, M. J. & Meszaros, P. 1994, *ApJL*, 430, L93
13. Spada, M., Ghisellini, G., Lazzati, D., & Celotti, A. 2001, *MNRAS*, 325, 1559
14. Takahashi, T. et al. 2000, *ApJL*, 542, L105
15. Tanihata, C., Takahashi, T., Kataoka, J., & Madejski, G. 2003, *ApJ*, in 584, 153